MASS TRANSFER IN THE CORNEA

II. Ion Transport and Electrical Properties of a Series Membrane Tissue

M. H. FRIEDMAN

From the Applied Physics Laboratory, The Johns Hopkins University, Silver Spring, Maryland 20910

ABSTRACT The electrical and active transport properties of isolated rabbit cornea are investigated by computer experimentation. The tissue is modeled as a series membrane system and the passive ion fluxes through it are described by the frictional formulation of irreversible thermodynamics. From short-circuit current (SCC) data, it is found that the epithelial sodium pump rate (P) is not appreciably changed when much of the sodium in the solution bathing the anterior corneal surface (concentration = c_{11}) is replaced by choline, with choline-free medium posteriorly. Simulations of open-circuited corneas, using the mean P computed from the SCC data, yield corneal and stromal potentials in agreement with experiment. The stromal fluid is calculated to become more hypotonic as c_{11} is diminished, a result consistent with posttest measurements of the sodium content of experimental stromata. The apparent decrease in "bound sodium" which accompanies the reduction of c_{11} is a result of the associated changes in steady stromal hydration; the epithelial sodium pump does not contribute to corneal deturgescence. The inclusion of a simple epithelial structure in the computations changes the value of P but affects neither its constancy nor the calculated behavior of the cornea under open-circuit conditions. A general algebraic relation among pump rates and ion fluxes in short-circuited series membrane systems bathed in complex media is derived and used to construct a relation between P and SCC for the cornea. This equation yields pump rates in good agreement with the computer results and is used to show that (*a*) P is independent of c_{11} if $d(SCC)/dc_{11}$ is a constant related to the over-all corneal permeability to sodium, and (*b*) a Lineweaver-Burke plot of $1/SCC$ vs. $1/c_{11}$ can appear to be linear at constant P.

INTRODUCTION

An established method for quantitating the transport properties of biological structures is that of making electrical measurements on the tissue. These measurements can sometimes be interpreted quite easily; for instance, if a simple membrane actively transports a single ion through a "path" which excludes all other species, the short-circuit current (SCC) when the membrane is bathed by identical solutions on both surfaces is indeed the pump current. Real systems, however, are often not

so simple, with the important consequence that the pump rate (P) cannot always be identified with the SCC. Most tissues are complex in structure, and short circuiting of the entire system gives no assurance that the potential drop across the pump is zero (Rehm, 1968). Furthermore, in studies of the influence of ambient composition and substrate concentration on pump rate, the individual tissue surfaces are often exposed to different solutions, and the consequent passive diffusion of permeating species further obscures the relation between P and SCC.

On the other hand, if the transport properties of the solutes in the tissue are known, and the pump site and substrate identity are postulated, there is no reason in principle why the pump rate should not be recoverable from the electrical properties of the tissue, short-circuited or not. The flux equations may still be written, but their solution is not explicit. Thus, computer modeling becomes an attractive technique for studying biological structures in generally complex environments.

A computer model of the cornea is used here to examine the implications of Green's (1968, 1969) measurements of the variation of the SCC of the isolated rabbit cornea as the sodium content of the medium bathing both surfaces is replaced in part by potassium and as the sodium bathing the epithelial surface is further replaced by choline. Both short-circuited and open-circuited corneas are examined by this technique. It is shown that the species fluxes through the short-circuited cornea may be described analytically, in spite of the complexities of structure and environment which are involved. Computer modeling is still necessary in cases where the potential across the tissue is not reduced to zero by the passage of an external current.

The approach used here is of course not limited in application to the cornea. In the course of this work, general relations between the SCC and the properties of series membrane systems possessing multiple pumps are developed. These are used here to examine the influence of epithelial structure (pump site, distribution of passive resistances) on the conclusions of short-circuit experiments. The relation between pump rate and the SCC is examined in detail using a Nernst-Planck description of the passive fluxes, and briefly in terms of a formal irreversible thermodynamic treatment which includes metabolic coupling.

SYMBOLS

All symbols are defined where they first appear. Because of their large number, a listing would nonetheless appear to be desirable for clarity. Symbols which are defined simply as collections of other variables (i.e., the π's and α's following equations 1) are omitted.

A Affinity.

a Membrane thickness; a_k = thickness of the kth membrane ($k = 1$ is epithelium, $k = 2$ is endothelium, $k = 1a$ is anterior membrane of structured epithelium, $k = 1p$ is posterior membrane of structured epithelium).

c_j Concentration of the jth species ($j = 1$ is sodium).

c_{j1} Concentration of the jth species in the epithelial bath ($j = 1$ is sodium) or on one side of a series membrane system.

c_{j3} Concentration of the jth species in the endothelial bath ($j = 1$ is sodium).

c_{ja} Average of the concentrations of the jth species in the solutions bounding the stroma.

c_{jk} Concentration of the jth species between the kth and $(k + 1)$st membranes in a series membrane system.

$c_{j,K+1}$ Concentration of the jth species on the side of a series membrane system opposite to c_{j1}.

$\bar{c}_j$ Concentration of the jth species in the epithelial and endothelial baths when $c_{j1} = c_{j3}$.

c_j^* Total stromal concentration of the jth species, stromal fluid basis.

F Faraday's number.

f_j Friction coefficient measuring membrane and solvent drag on the jth species ($j = 1$ is sodium, $j = 2$ is choline; $f_{jk} = f_j$ in the kth membrane ($k = 1$ is epithelium, $k = 2$ is endothelium, $k = 1a$ is anterior membrane of structured epithelium, $k = 1p$ is posterior membrane of structured epithelium).

H Stromal hydration.

I Observable current density.

J_j Passive flux of the jth species ($j = 1$ is sodium); $J_{jk} = J_j$ in the kth membrane.

K Number of membranes in a series membrane system.

L_j, L_{jr} Phenomenological coefficients ($j = 1$ is sodium).

N Total concentration $= \sum_j c_j$; $N_k = \sum_j c_{jk}$.

n Number of permeable ions.

P Epithelial pump rate.

P_{jk} Pump rate of the jth species in the kth membrane ($k = 1$ is epithelium, $k = 2$ is endothelium).

R_k Resistance of the kth membrane ($k = 1$ is epithelium, $k = 2$ is endothelium, $k = 1a$ is anterior membrane of structured epithelium, $k = 1p$ is posterior membrane of structured epithelium).

R Gas constant.

$\bar{R}$ Resistance coefficient measuring interactions between oppositely charged ions; $\bar{R}_k = \bar{R}$ in the kth membrane.

T Absolute temperature.

X Membrane charge density.

X_j Gross flux of the jth species ($j = 1$ is sodium, $j = 2$ is choline).

x Distance coordinate normal to membrane surface.

z_j Valence of the jth species.

z_x Sign of membrane charge (± 1).

α Short-circuit current (SCC).

γ_j Activity coefficient of the jth species.

$\tilde{\mu}_j$ Electrochemical potential of the jth species ($j = 1$ is sodium).

ψ Electrostatic potential; when not superscripted, corneal potential.

ψ_D Donnan potential.

Superscripts

a, b Two faces of a single membrane (in equations 1 only).

a, p Active and passive pathways, respectively; in Fig. 5, anterior and posterior stroma, respectively.

$'$, $''$ Two phases in Donnan equilibrium.

THE EXPERIMENTAL SYSTEM

The corneal model is shown in Fig. 1. The cornea consists of three principal layers, each covering the entire corneal area; from anterior to posterior, these are the epithelium, the stroma, and the endothelium. In vivo, the epithelium is bathed by the tears and the endothelium is bounded posteriorly by the aqueous contained in the anterior chamber of the eye. The corneal diameter is about 20 times its thickness so, for mathematical purposes, each layer may be regarded as infinite in extent. The epithelium and the endothelium are cellular layers. It is generally accepted (Donn et al., 1959; Green, 1967; Ehlers and Ehlers, 1968) that the SCC of the cornea arises from a sodium pump in the epithelium; pumping is from the tear film towards the stroma. The stroma is nearly acellular and is normally about 75% water by weight; the remainder of this open structure is comprised of a rather regular array of collagen fibers, presumably connected via mucopolysaccharide chains. The mucopolysaccharides contain dissociated acid moieties, only a fraction of which are neutralized by bound counterions, and the stroma consequently bears, under normal conditions, a net negative charge (Catchpole et al., 1966; Otori, 1967; Friedman and Green, 1971). It therefore behaves in some respects as a polyelectrolyte gel and, as such, possesses the ability to swell. Since the stroma is charged, the anteriormost stromal fluid is in Donnan equilibrium with that at the posterior epithelium; a similar equilibrium obtains at the stroma-endothelium interface (see, for instance, Teorell, 1953).

The model properties of the rabbit cornea and the references or techniques used in their evaluation are given in Table I. The permeability properties of the corneal layers are measured by two sets of phenomenological coefficients: f_{jk}, a friction coefficient (Kedem and Katchalsky, 1961) which measures the drag on a mole of j traversing the kth corneal layer, and arising from j's velocity relative to the membrane and solvent water (the solvent is assumed to be stationary relative to the cornea; arguments to support this assumption in the present work are presented subsequently); and $\bar{R}_k$, the generalized resistance coefficient measuring direct interactions between oppositely charged ions in the kth layer. The same value of $\bar{R}_k$ is assumed to obtain for all pairs of oppositely charged ions in the kth layer and direct interactions between ions of like charge are ignored.

Table II gives the composition of the solutions bounding the cornea and the values of SCC

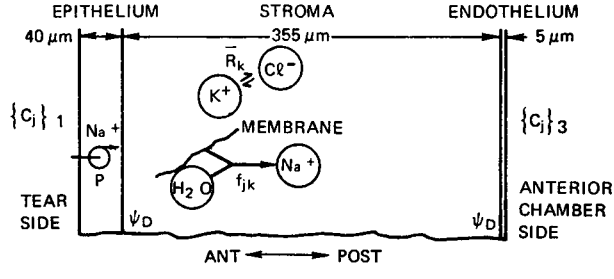

FIGURE 1 Model cornea. P is the epithelial sodium pump rate; ψ_D represents the Donnan potential between the stroma and the (presumably) uncharged adjacent phases. The two sketches inside the stroma show the two kinds of interactions considered here: the drag on ions, such as sodium, by membrane and solvent, measured by f_{jk}; and the interaction between oppositely charged ions, such as potassium and chloride, measured by $\bar{R}_k$. These interactions are presumed present in all corneal layers. The compositions of the epithelial and endothelial baths in the in vitro experiments to be analyzed here are given by $\{c_j\}_1$ and $\{c_j\}_3$, respectively.

TABLE I

PROPERTIES OF MODEL RABBIT CORNEA

Corneal temperature = 298°K.

Property	Membrane		
	Epithelium	Stroma	Endothelium
$\bar{R}$*, *J-sec-cm/mole²*	-1.91×10^{13}‡	-2.65×10^{11}§‖	-3.37×10^{12}‡
f_{Na}¶, *J-sec/mole-cm²*	7.94×10^{11}**	3.78×10^{8}§‖	4.06×10^{11}§‖
f_{Cl}	5.22×10^{11}‡‡	3.08×10^{8}§‖	2.68×10^{11}§‖
$f_{\bar{x}}$	5.41×10^{11}‡‡	2.58×10^{8}‡‡	2.79×10^{11}‡‡
f_{HCO_3}	8.95×10^{11}‡‡	5.28×10^{8}§§	4.59×10^{11}§§
f_{Ch}	1.38×10^{13}‖‖	5.28×10^{8}¶¶	1.15×10^{12}‖‖
Thickness, *cm*	4×10^{-3}*** ‡‡‡	3.55×10^{-2}*** ‡‡‡ §§§	5×10^{-4}***
Charge density, *meq/l fluid*	0	-38‖‖‖	0

* Phenomenological resistance measuring direct interactions between oppositely charged ions. $\bar{R}$ and f_j (¶ below) are defined by $-d\bar{\mu}_j/dx = -\sum_{i(z_i=-z_j)} \bar{R}(J_j c_i/c_j - J_i) + f_j J_j/c_j$ where i and j index the ions, $\bar{\mu}$ is electrochemical potential, x is distance through the membrane, z is ionic charge, J is passive flux, and c is concentration.

‡ Donn et al. (1963) measured the self-diffusion of HTO through the corneal membranes. Their data were used to estimate the effective membrane tortuosity, which was then used to obtain the needed $\bar{R}$ from the pure saline data in §. The value of $\bar{R}$ given here is likely to be an overestimate; in any event the influence of ion-ion interactions is small in the epithelium and endothelium, where the solute-membrane interaction is large.

§ Katchalsky and Curran (1965). The value of $\bar{R}$ in the stroma is found from that in saline.

‖ Maurice (1961) gives the obstruction of stroma and endothelium to diffusion; this obstruction applied to known friction coefficients (§) in saline.

¶ Phenomenological friction coefficient (Kedem and Katchalsky, 1961) measuring solvent and membrane drag. See * for defining equation.

** Green (1967). Tracer measurement.

‡‡ Based on friction coefficient of sodium, assuming f_j inversely proportional to limiting mobility at infinite dilution; mobility values u^0 from Edsall and Wyman (1958). The equation used is $f_{HCO_3} = f_{Na} u^0_{Na}/u^0_{HCO_3}$, f_{Na} from Green (1967).

§§ Similar to ‡‡; based on friction coefficient of chloride. The equation used is $f_{HCO_3} = f_{Cl} u^0_{Cl}/u^0_{HCO_3}$, f_{Cl} from Maurice (1961).

‖‖ Green, K. Private communication. Tracer measurement.

¶¶ Friction coefficient of choline equated to that of bicarbonate.

*** Maurice (1962).

‡‡‡ Trenberth and Mishima (1968).

§§§ The stromal thickness used throughout is the normal value, though in some of the experiments modeled here, the cornea was swollen. The stroma is so permeable that the electrical properties of the entire cornea are essentially independent of stromal thickness over the range of interest (Friedman and Kupfer, 1960).

‖‖‖ This value derives from some early measurements of stromal sodium content since incorporated in Green et al. (1971). A more thorough analysis of these and additional data (Friedman and Green, 1971), carried out contemporaneously with the work reported here, showed that a value of -12 to -16 meq/l more correctly represents the stromal charge density at normal hydration. For consistency, the earlier value was retained throughout the present work. The only effects of any consequence of the overestimate of stromal charge density are on the Donnan potential and base line stromal tonicity; these are dealt with in the text.

measured by Green (1968, 1969). The basic medium used by Green was Ringer's solution, which is more complex than those in Table II, where only the major ionic species are given. All species not in Table II were always present in the same equal amounts on both corneal surfaces and their omission from the computer model is not expected to affect its behavior.

TABLE II

BATHING SOLUTIONS AND SHORT-CIRCUIT CURRENT (SCC)

Case	Epithelial bath	Endothelial bath	SCC
			*eq/cm²-sec**
1	I‡	I	1.111×10^{-10}
2	II_0§	II_0	9.73×10^{-11}
3	II_{18}	II_0	6.95×10^{-11}
4	II_{53}	II_0	5.00×10^{-11}
5	II_{98}	II_0	2.78×10^{-11}
6	II_{118}	II_0	1.111×10^{-11}

* Positive ion flux, tears to aqueous.
‡ Solution I (meq/l): Na, 143; Cl, 123; K, 5; HCO_3, 25.
§ Solution II_x (meq/l): Na, (118-x); Cl, 123; K, 30; HCO_3, 25; choline, x.

The SCC values do not reflect Green's experimental precision; the "insignificant" digits in Table II are a consequence of converting his results to cgs units.

MATHEMATICAL METHODS

In modeling the cornea, the compositions of the bounding solutions are known ($\{c_j\}_1$ and $\{c_j\}_2$; see Fig. 1). The permeable ions are pumped or pass through all three corneal layers; in the steady state, for the jth ion, the gross species flux X_j is the same in each layer. The gross flux X_j equals $J_{jk} + P_{jk}$, where J_{jk} and P_{jk} are the passive and pump fluxes of j through the kth corneal layer. The problem to be solved is this: Given the compositions of the bounding solutions, the properties of the corneal layers, the observable current density, and the site, rate, and substrate of any assumed metabolic pumps, what are the membrane potentials and what are the fluxes and internal concentrations of each of the mobile ions?

To carry out the calculation, two classes of solutions were developed. In a multi-ionic system in which activity coefficient gradients are negligible, the passive fluxes and potential across a single membrane are given by (Friedman, 1970)

$$c_j^b = e^{-u_j^b}(u_j^b)^{-\pi_{3j}}\left\{\frac{1}{\pi_1^2}[U_j(u_j^b) - U_j(u_j^a)] + e^{u_j^a}(u_j^a)^{\pi_{3j}}c_j^a\right\}, \qquad (1\,a)$$

$$\frac{a}{RT} = -\frac{1}{\bar{R}J_{+j}}(u_j^a - u_j^b) + \frac{\pi_2}{\pi_1^2}\ln\frac{u^b}{u^a}, \qquad (1\,b)$$

$$F(\psi^b - \psi^a) = \bar{R}I'a + \frac{RT\pi_2}{\pi_1 z_x X}\ln\frac{u^b}{u^a}, \qquad (1\,c)$$

where $u_j = -\bar{R}J_{+j}(\pi_2 + N\pi_1)/\pi_1^2$, $\pi_{3j} = \pi_2[\bar{R}J_{+j} + \pi_1 z_j/(z_x X)]/\pi_1^2$, $\pi_1 = \sum_j f_j J_j -$

$\bar{R}z_xXI'$, $U_j(u) = u^{\pi_{3j}}\{\Gamma(\pi_{3j})\gamma^*(\pi_{3j}, -u)[\alpha_{0j} - \alpha_{1j}\pi_{3j} + \alpha_{2j}\pi_{3j}(\pi_{3j} + 1)] + \exp(u)[\alpha_{1j} - \alpha_{2j}(\pi_{3j} + 1 - u)]\}$, a is membrane thickness, R is the gas constant, T is absolute temperature, J_{+j} is the total passive flux of ions charged similarly to $j(\sum_{i(z_i=z_j)} J_i)$, $\pi_2 = z_xX\sum_j J_jz_jf_j - \bar{R}X^2J$, F is the Faraday, ψ is potential, $I' = \sum_j J_jz_j$ is diffusion current density, z_x and X are the sign and density respectively of the membrane charge, $N = \sum_j c_j$, z_j is the charge on the (assumed monovalent) jth ion, Γ is the gamma function, γ^* is the incomplete gamma function, $\alpha_{0j} = \pi_2[-\bar{R}J_j\pi_2/(2\pi_1) - \pi_{4j}]$, $\alpha_{1j} = -\pi_1(\pi_{4j}\pi_1/\bar{R} + J_j\pi_2)/J_{+j}$, $\alpha_{2j} = -J_j\pi_1^2/(2\bar{R}J_{+j}^2)$, $J = \sum_j J_j$, $\pi_{4j} = J_jf_j - \bar{R}J_jz_xz_jX/2$, and the superscripts a and b denote the two (interior) faces of the membrane.

This solution was developed for the case in which convective effects on the flow of ions is negligible; there are a number of lines of evidence which suggest that this condition may be assumed for the present study. Cereijido and Curran (1965) found from freezing-point depression measurements that the osmotic activity of choline-containing Ringer's solution, nominally isotonic to normal Ringer, was approximately the same as that of the latter. Green's measurements of SCC and corneal potential were made without a hydrostatic pressure head across the clamped cornea. His measurements (1969) of the steady thickness and stromal ion content of corneas subjected to compositional variations identical with those used in the electrical studies were carried out under 20 cm H_2O simulated intraocular pressure (IOP). Since these data will be referred to below, it is worth noting that Edelhauser et al. (1968) and Donn et al. (1963) measured the unidirectional fluxes of HTO across isolated corneas and found no measurable bulk flow in the steady state under zero (presumably) and 5–35 cm H_2O simulated IOP, respectively. Occasional measurements of transcorneal potential under simulated IOP showed no influence of hydrostatic pressure on this electrical property, so long as the corneal membranes were undamaged (Green, private communication).

The compositions of the solution phases at the two sides of an interface separating membranes having differing charge densities are related by the Donnan equilibrium condition. For the cornea, this condition must be applied at the stromal surfaces. So that the computational scheme could be used for other series membrane systems, a very general Donnan equilibrium routine was coded, which included ion activity coefficients and allowed for the possibility that both membranes at the interface might be charged. The derivation of this general interface condition is given in Appendix I; the final equation is

$$c_j'' = \zeta_j E^{-z_j/z_{x''}}, \tag{2 a}$$

where

$$E = \frac{X'' + \{[X'']^2 + \Gamma_{g''}\Gamma_{c'}[(N')^2 - (X')^2]\}^{1/2}}{\Gamma_{g''}(N' + z_{x'}z_{x''}X')}, \tag{2 b}$$

and where the primes denote the two phases in equilibrium, $\zeta_j = \gamma_j' c_j'/\gamma_j''$, $\Gamma_{a'}$ (or $\Gamma_{c'}$) $= \gamma_j'/\gamma_j''$ for the ions for which $z_j = -z_{x'}$ (or $z_j = z_{x'}$), and γ_j is the activity coefficient of the jth ion.

In application to the cornea, the input to the simulator consisted of the membrane parameters (Table I), the bounding solution compositions (Table II), a proposed epithelial sodium pump rate P, and the observable current density $I = \sum_j z_j X_j$. The values of X_j and the corresponding transmembrane potentials and intracorneal compositions were found using a root finder (Brown and Conte, 1967) for the X_j.

The procedure may be illustrated with reference to Fig. 1. Consider that there are n permeable ions. The root finder constructs a trial set of $(n - 1)$ X_j's; X_n is then found from I. The composition of the epithelial bath is known, and the epithelial surface is regarded as plane a in equations 1. The trial values of X_j replace J_j in these equations, except for sodium (subscript 1), for which $J_1 = X_1 - P$. Equations 1 then give $\{c_j^b\}$, the composition at the posterior epithelium (the subepithelial solution), and $\psi^b - \psi^a$, the transepithelial potential. The Donnan equilibrium condition (equations 2), with the primed phase representing the subepithelial solution, is used for $\{c_j''\}$, the composition of the stromal fluid at the anterior stromal surface; the Donnan potential is found as well. Equations 1 are now used to cross the stroma (c_j^a = anterior stroma, c_j^b = posterior stroma, $J_j = X_j$ because no pumps are sited in the stroma or endothelium). Equations 2 describe the Donnan equilibrium at the posterior stroma (c_j' = posterior stroma, c_j'' = anterior endothelium, the supraendothelial solution); and equations 1 are used to cross the endothelium (c_j^a = supraendothelial solution, c_j^b = endothelial bath, $J_j = X_j$). The root finder seeks the values of $\{X_j\}$ such that the values of c_j^b calculated in this last step are identical with the known composition of the endothelial bath, $\{c_j\}_3$. It will be observed that, with this procedure, the intracorneal compositions and all potentials of interest are also found, *en passant*.

The gradients in ionic strength across and within the cornea are small, so the assumption implicit in equations 1 that activity coefficient gradients within a membrane can be neglected is justified. In using equations 2 at the stromal interfaces, the activity coefficient ratios given by the Γ's were set equal to unity on similar grounds: the bound counterions are not counted in c_j and the effect of the small stromal charge is to change the activity coefficients and the ionic strength of the stromal fluid only slightly from their values in an equilibrium, electrically neutral solution (Friedman and Green, 1971).

RESULTS AND DISCUSSION

Short-Circuit Behavior and Epithelial Pump Current

As noted above, for simple membranes bathed by identical media on both surfaces, P = SCC. When this identity was applied to the data in Table II by setting I = SCC and using a trial pump rate equal to SCC, the computed corneal potential ψ ranged

from −0.6 mv (case 2) to −10.1 mv (case 6), endothelial side negative. If the trial pump rate had been the true rate, then ψ would have been zero. For cases 1 and 2, where identical solutions bathed both corneal surfaces, the evident difference between the true P and SCC is a consequence of the series membrane structure of the cornea; when choline is added to the epithelial bath (cases 3–6), this difference is further increased because the cornea is more permeable to sodium than to choline, and the concentration gradient of the former drives an anteriorly directed passive sodium flux which contributes to the measured SCC.

Next, the short-circuit case was again reproduced by setting I equal to SCC, and the true epithelial pump rate was found as that value of P such that the calculated ψ *was* zero. These values and the SCC are plotted in Fig. 2 against the sodium content of the epithelial bath. It can be seen that there is no evidence that the epithelial pump rate is sensitive to the sodium content of the epithelial bath over the range of compositions studied. The average value of P, based on the computer results for cases 1–4 and 6, is $(10.3 \pm 0.6) \times 10^{-11}$ eq/cm^2-sec.

From these and other similar computer experiments, it was seen that the value of the pump rate found in this way was little affected by neglecting ion-ion interactions or omitting the highly permeable, lightly charged stroma from the calculation. The cornea can then be described as an epithelium and an endothelium in series. A general relation among pump and passive fluxes through a short-circuited assembly of K uncharged membranes in series, in the absence of ion-ion interactions, and under compositional boundary conditions with which Green's experiments are consistent, is (Appendix II)

$$c_{j,K+1} - c_{j1} = \frac{2}{N_1}\left[\sum_{k=1}^{K} s_{jk}(N_1 + S_k) + 2\sum_{k=2}^{K} s_{jk}\sum_{l=1}^{k-1} S_l\right], \tag{3}$$

where $\{c_j\}_1$ and $\{c_j\}_{K+1}$ are the compositions of the isotonic ($N_1 = N_{K+1}$) bathing media, $s_{jk} = (P_{jk} - X_j)f_{jk}a_k/(2RT)$, and $S_k = \sum_j s_{jk}$. For the case in which there is only one pump, $P = P_{j'k'}$, this set of coupled second-degree equations can be made linear in P to facilitate its calculation from the SCC (Appendix II):

$$c_{j,K+1} - c_{j1} = \frac{2}{N_1}\left[\delta_{k'>1}\sum_{k=1}^{k'-1} s_{jk}\left(N_1 + S_k + 2\sum_{l=0}^{k-1} S_l\right)\right.$$
$$\left. + s_{jk'}\left(N_1 + \sum_{l=0}^{k'-1} S_l - \sum_{l=k'+1}^{K+1} S_l\right) + \delta_{k'<K}\sum_{k=k'+1}^{K} s_{jk}\left(N_1 + S_k - 2\sum_{l=k}^{K} S_l\right)\right], \tag{4}$$

where $S_0 \equiv 0$, $S_{K+1} \equiv 0$, and $\delta_{k'>1}$ ($\delta_{k'<K}$) is unity if $k' > 1$ ($k' < K$) and zero if $k' = 1$ ($k' = K$). For a cation not actively transported, s_{jk} is proportional to X_j. If this species is present in equal amounts on both sides of the membrane system, both sides of equation 4 are zero, consistent with $X_j = 0$.

For the simplified representation of the cornea as an epithelium ($k = 1$) and endothelium ($k = 2$) in series, the only species whose fluxes are nonzero under

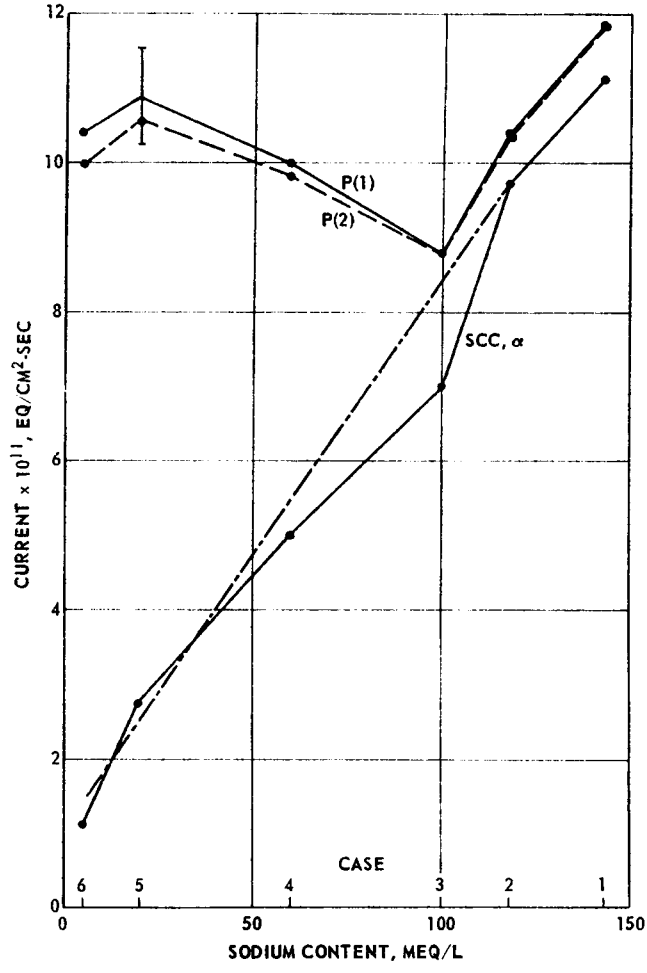

FIGURE 2 Measured short-circuit current (SCC, α) and computed epithelial pump current (P) vs. sodium content of the epithelial bath. $P(1)$, ———, based on computer experiments. Convergence difficulties permitted only a range of values of P to be found for case 5. $P(2)$, — — —, based on limiting solution, equation 7. — — —; linear relation between α and c_{11} given by equation 9 b, c_{13} = 118 meq/l.

short-circuit conditions are sodium ($j = 1$) and choline ($j = 2$); here $K = 2$, $k' = 1, j' = 1$, and equation 4 becomes

$$c_{j3} - c_{j1} = 2[(s_{j1} + s_{j2})(N_1 - S_2)]/N_1. \quad (5)$$

Substituting the definitions of s_{jk}, with SCC $\equiv \alpha = X_1 + X_2$, this gives, for $j = 1$

$$c_{13} - c_{11} = \frac{2}{N_1}[(PF_{11} + X_2F_{11} - \alpha F_{11} + X_2F_{12} - \alpha F_{12}) \cdot (N_1 - X_2F_{12} + \alpha F_{12} + X_2F_{22})], \quad (6)$$

where $F_{jk} = f_{jk}a_k/(2RT)$.

The epithelium is considerably less permeable to choline than to sodium (Table I);

it is instructive to examine the limiting case, $X_2 \ll \alpha$. Since the endothelial permeabilities to the two species are comparable, $X_2F_{22} \ll \alpha F_{12}$ and equation 6 simplifies to give, upon rearrangement,

$$P = \frac{1}{F_{11}}\left[\alpha(F_{11} + F_{12}) - \frac{N_1(c_{11} - c_{12})}{2(N_1 + \alpha F_{12})}\right]. \quad (7)$$

The first term in the brackets shows how the relation between P and SCC is affected by the series membrane nature of the cornea, and the second term measures the influence of transcorneal concentration gradients, for this limiting case. When equation 7 is used to calculate the pump current from the experimental values of SCC, good agreement with the computer experiments is observed (Fig. 2).

Open-Circuit Behavior: Corneal Potential and Ion Fluxes

Next, cases 1–6 were simulated under open-circuit conditions ($I = 0$) with $P = 10.3 \times 10^{-11}$ eq/cm^2-sec, to give ψ. The transcorneal and transepithelial potentials

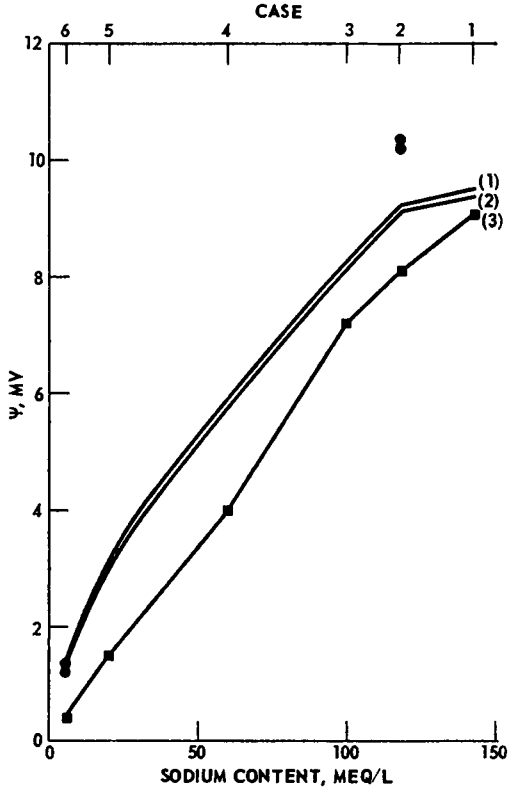

FIGURE 3 Open-circuit corneal potential (ψ) vs. sodium content of the epithelial bath. (1) Computed transepithelial potential. (2) Computed transcorneal potential. For 1 and 2, epithelial pump rate = 10.3×10^{-11} eq/cm^2-sec. ●, computed transepithelial (upper) and transcorneal (lower) potentials when epithelium structured. (3), ■, experimental transcorneal potential.

are shown in Fig. 3; the difference between the two is the (negative) transendothelial potential. Because of the ease with which the stroma passes ions, the osmotic gradient across this structure is small and the stromal contribution to the corneal potential is negligible. Also given in Fig. 3 are the measured in vitro transcorneal potentials, for each case (Green, private communication). Recognizing that the simulator calculation of ψ is based on the measured properties of the corneal membranes and on a value of P calculated from other experimental data, the agreement in Fig. 3 is really quite good. Clearly, the epithelium is the dominant source of the corneal potential. The decrease in transcorneal potential when sodium in the epithelial bath is replaced by choline has also been observed by Muneoka (1967) and for beef cornea by Lindemann (1968). The calculated transcorneal potential is most sensitive to F_{11}; the value of F_{11} used here is based on Green's (1967) permeability measurements. Green's epithelial sodium permeability has been challenged by Maurice (1967) as being too high, possibly as a result of experimentally induced trauma. The importance of epithelial sodium permeability will be discussed in some detail below;

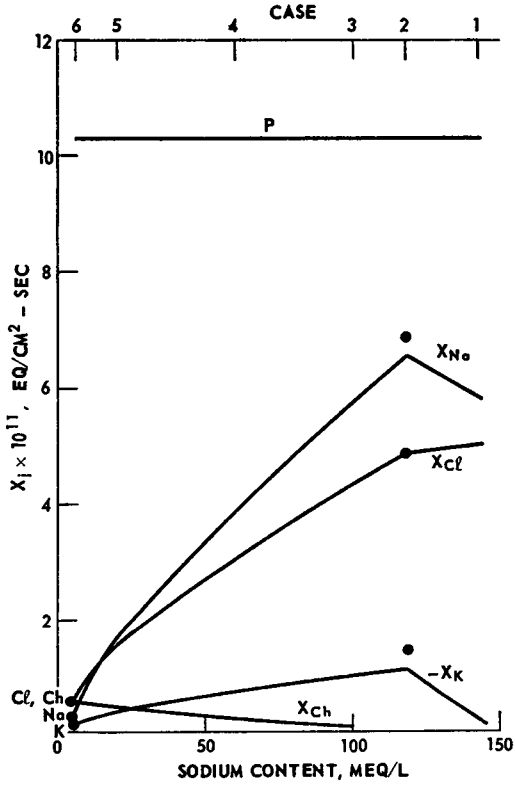

FIGURE 4 Open-circuit gross ion fluxes (X_j) vs. sodium content of the epithelial bath, X_{HCO_3} omitted for clarity. Constant pump rate $P = 10.3 \times 10^{-11}$ eq/cm²-sec is noted on the figure. ●, computed results when epithelium structured.

here it is sufficient to note that the potentials measured by Green are in any event consistent with his permeability measurement.

The stromal potential relative to the epithelial bath is given by the sum of the transepithelial potential and the Donnan potential at the epithelium-stroma interface. The Donnan potential in case 1 is -3.2 mv when the value of stromal charge density in Table I is used. A more recent value of charge density at normal hydration is (Friedman and Green, 1971) -14 meq/l, giving a Donnan potential of -1.2 mv and a corresponding stromal potential of $+8.3$ mv, in good agreement with the macroelectrode and microelectrode values of $+8.6$ and $+6.0$ mv obtained experimentally by Klyce and Zadunaisky (1970).

The gross fluxes X_j of the mobile ions through open-circuited corneas are plotted in Fig. 4. The concentrations of potassium and chloride in the ambient baths are the same on both sides of the cornea, $c_{j1} = c_{j3} \equiv \bar{c}_j$, so their fluxes are more or less proportional to $-z_j\bar{c}_j\psi$; the same is true of the bicarbonate flux, which has been omitted from Fig. 4 for the sake of clarity. The gross sodium flux falls as c_{11} is lowered, even though P is held constant and ψ is changing in a direction to favor the migration of this ion towards the endothelium. The decrease in sodium flux is a consequence of the considerable sodium concentration gradient which results when this species is removed from the epithelial bath. In case 6, in effect, 97% of the sodium pumped by the epithelium returns to the tear side by passive diffusion and migration.

Open-Circuit Behavior: Stromal Ion Content

Green (1968) found that as the sodium concentration in the epithelial bath was reduced, the cornea swelled to larger equilibrium thicknesses. This swelling was attributed to a reduction in epithelial pump rate. It is not clear how swelling would be induced by pumping *fewer* ions into the stroma and, in any event, it now appears that when the effects of concentration gradients are taken into account, P is substantially unaffected by the compositional variations which caused the cornea to swell.

Another possible explanation of the observed swelling is that the interaction of the active and passive fluxes through the cornea cause the stromal tonicity to rise as the composition of the epithelial bath is changed from normal Ringer. Fig. 5 shows how the calculated stromal osmolarity varies with the sodium content of the epithelial bath, under open-circuit conditions, and with $P = 10.3 \times 10^{-11}$ eq/cm^2-sec. The replacement of 25 meq Na by K on both corneal surfaces (case 2 vs. case 1) has a minor effect on the stromal osmolarity; however, continued replacement of sodium by choline on the epithelial side results in a *drop* in stromal osmolarity, even though no decrease in pump current is assumed.

The stromal osmolarity depends on the ionic content of the electrically neutral solutions[1] which bound the stroma and on the stromal charge density. By electro-

[1] By the "solutions which bound the stroma", the "stromal environment," and the "solution phases adjacent to the stroma," we refer to the electrically neutral subepithelial and supraendothelial solu-

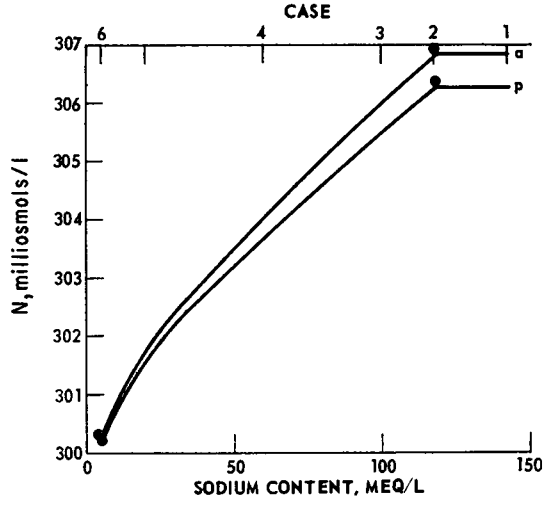

FIGURE 5 Stromal osmolarity vs. sodium content of the epithelial bath. Pump rate fixed at 10.3 × 10^{-11} eq/cm²-sec. *a*, anterior stroma; *p*, posterior stroma; ●, computed results when epithelium structured.

neutrality, the osmolarity of the stromal environment is simply twice the cation content of these solutions. Since the epithelium is only slightly permeable to choline, little of this species is found subepithelially. The potassium ion is a relatively minor component; furthermore, since $c_{K,1} = c_{K,3} \equiv 30$ mM in cases 2–6, its concentration at the posterior epithelium and anterior endothelium varies only slightly as the sodium content of the epithelial bath is reduced. Thus the principal composition variable affecting stromal osmolarity for cases 2–6 is the sodium content of the solutions bounding the stroma. Since the stroma is much more permeable to ions than are the other corneal layers, the gradients across this structure are small, and the compositions at the posterior epithelium and at the anterior endothelium differ only slightly. The excess of sodium at the anterior endothelium over that in the endothelial bath is that required to drive the posteriorly directed sodium flux across the endothelium. As the sodium content of the epithelial bath is diminished, the gross sodium flux (Fig. 4) and transendothelial sodium concentration gradient fall. The sodium content of the stromal environment accordingly decreases, since c_{13} is fixed. Hence the stromal osmolarity drops.

The charge density of the stroma affects its ion content only through the Donnan effect. The Donnan pressure of model stroma in equilibrium with a 148 mM solution is 2.4 milliosmols, so in the absence of pumping or concentration gradients across the cornea, the stromal osmolarity would be uniform at 298.4 milliosmols/l. The curves in Fig. 5 would be shifted vertically were a stromal charge density other than that in Table I used, but they would for all practical purposes be otherwise un-

tions which are in Donnan equilibrium with the anterior and posterior surfaces of the stroma, respectively.

changed. For instance, were the stroma uncharged, the curves in Fig. 5 would shift downward by 2.4 milliosmols/l.

The conclusion that a decrease in stromal tonicity accompanies the replacement of epithelial sodium by choline is consistent with Green's (1969) posttest measurements of the sodium content of the experimental stromata. The sodium concentrations measured by Green should differ from those in the solution phases adjacent to the stroma for two reasons. First, a certain amount of stromal sodium is bound to acid sites in the tissue; this bound sodium is included in Green's analyses but is not counted in c_1. Second, the free stromal charge gives rise to a Donnan excess of mobile sodium ions in the stroma. Friedman and Green (1971) have shown that on a dry tissue basis, the concentrations of bound sodium and free stromal charge (milliequivalents per kilogram dry tissue) are nearly independent of stromal hydration, H grams fluid per gram dry tissue. Thus, when these concentrations are expressed in milliequivalents per kilogram fluid for consistency with the present work, they are seen to be inversely proportional to hydration. The free site concentration is much less than the osmolarity of the solutions bounding the stroma, so the Donnan sodium excess is simply proportional to the concentration of free acid sites. Thus $(c^*_{Na} - c_{Na,a}) \propto 1/H$, where c^*_{Na} is the total concentration of stromal sodium, as measured by Green, and $c_{Na,a}$ is taken to be the average of the subepithelial and supraendothelial sodium concentrations.

In Fig. 6, $c^*_{Na} - c_{Na,a}$ is plotted against the reciprocal of the hydration to which the corneas swelled in each case; c^*_{Na} is Green's experimental value (c^*_{Na} for case 2 is a private communication) and $c_{Na,a}$ is obtained from the computer simulations. Case 1 is not included in the figure to obviate any assumptions regarding the selectivity of the binding sites for sodium vis-à-vis potassium. It is seen that the data presented in this form can be fit by a straight line within the error bars. If $c_{Na,a}$ is assumed to be constant to variations in c_{11}, such linearity no longer obtains.

The size of the error bars in Fig. 6 is such that this observation does not prove that stromal tonicity decreases as c_{11} is diminished. Nonetheless, the c^*_{Na} data *are* fit better when the values of $c_{Na,a}$ given by the computer experiments are used. Perhaps more important, it is evident that the decrease in $c^*_{Na} - c_{Na,a}$, as c_{11} is diminished, can be explaimed completely as a result of the swelling which accompanies this change in the composition of the epithelial bath. There is no evidence for any causal influence of bound sodium on steady hydration.

In summary, then, the simulations discussed above indicate that the epithelial sodium pump rate is insensitive to considerable variations in the sodium content of the epithelial bath, and that the stromal fluid becomes more hypotonic as c_{11} is diminished, even in the absence of a concomitant decrease in the pump rate.

The Consequences of Epithelial Structure

In all the work presented above, the epithelium was modeled as a single membrane with the properties given in Table I. This is obviously a simplification, and one may

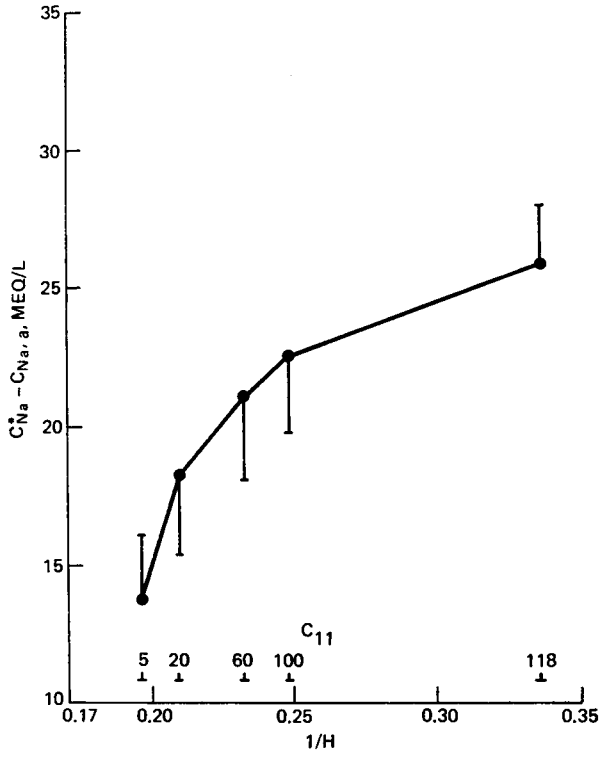

FIGURE 6 Stromal sodium excess vs. reciprocal hydration. The 1-SEM error bars correspond to the uncertainty in c^*_{Na}. The corresponding values of the sodium content of the epithelial bath are given on the abscissa.

fairly question the physical relevance of the results so obtained. In this section, the implications of a first-approximate epithelial structure will be compared with the conclusions which followed from the gross ("zeroth approximation") description employed above.

The epithelium is described to a first approximation by four membranes or regions in series. From anterior to posterior, they are: cell membrane (representing anterior epithelial surface), intracellular space, cell membrane (representing lateral and basal cell surfaces), and extracellular space in contact posteriorly with the stroma. Parallel paths through the epithelium are not modeled explicitly though they may be averaged in the resistance values assigned to each series layer. The resistances assigned to the intracellular and extracellular spaces are low, corresponding to equivalent electrolyte solutions, so in essence the first-approximate structure has all solute passing through two epithelial cell membranes in series. In the absence of any present evidence one way or the other, the sodium pump is sited in the posterior cell membrane, pumping into the extracellular space, in analogy with Ussing's (1960) organization of frog skin epithelium and Leaf's (1960) toad bladder.

According to Klyce and Zadunaisky (1970), one-half of the corneal resistance is across the outer surface of the epithelium when the tissue is incubated in normal media. Neglecting direct ion-ion interactions, the membrane resistance, R_k, is given by $R_k = a_k[\sum_j c_j/f_{jk}]^{-1}/F$. The values of f_{jk} and a_k are taken from Table I and used with the composition of normal medium (Table II, solution I), to compute the epithelial (R_1) and endothelial (R_2) resistances in Ringer's solution. Since the stromal resistance is negligible, $R_{1a} = (R_1 + R_2)/2$ and $R_{1p} = R_1 - R_{1a}$, where the subscripts a and p denote the anterior and posterior membranes of the structured epithelium. The thicknesses a_{1a} and a_{1p} are set equal to 80 A; $f_{j,1a}$ and $f_{j,1p}$ are computed from R_{1a} and R_{1p} by assuming that the friction coefficients of the several ions are in the same proportion to one another in each of the membranes of the structured epithelium as they are in the gross epithelium whose properties are given in Table I.

Only cases 2 and 6 were repeated using a structured epithelium, these being sufficient to establish the effect of this modification. The pump rate is higher than that found when the epithelium is modeled as a single membrane, and it is again independent of the sodium concentration in the epithelial bath (case 2, $P = 2.22 \times 10^{-10}$ eq/cm^2-sec; case 6, $P = 2.26 \times 10^{-10}$ eq/cm^2-sec). The pump rate, as calculated from the SCC, is higher here because a smaller fraction of the corneal resistance is shunted by the actively transporting membrane. This observation emphasizes the importance of structural effects (i.e., the arrangement of pumps and membranes) on the relation between P and SCC, even when both sides of the tissue are bathed by identical solutions. The open-circuit behavior of the cornea is essentially unaffected by epithelial structuring (Figs. 3–5).

Klyce and Zadunaisky's (1970) microelectrode profiles of rabbit corneal epithelium showed two potential plateaus, suggesting a more complex model consisting of one additional intracellular space and one additional resistive membrane. Such a model was not tried, because of the even more uncertain partition of the diffusional resistances which would have been necessitated. To the extent to which the first-approximate model is arbitrary, the conclusion to which it leads, that structuring does not affect the predicted open-circuit behavior, holds irrespective of the structural model employed, provided that the corresponding pump rate is used.

On the Apparent Constancy of the Epithelial Sodium Pump

The preceding analysis leads to the conclusion that the rate of active sodium transport in the rabbit corneal epithelium is independent of the substrate content of the epithelial bath, over the range studied. This result was unexpected and demands further discussion. In this section, possible sources of error will be discussed; the relationships among P, SCC, and the compositions of the ambient baths will be examined more generally; and the apparent insensitivity of P to c_{11} will be interpreted in terms of the irreversible thermodynamics of coupled metabolic activity and active transport.

A critical feature of the conclusion under consideration here is its reliance on the magnitudes of a number of corneal variables whose values have not been quantitatively reproduced by a large number of investigators. These include, most particularly, corneal SCC as a function of ambient composition, and epithelial solute permeabilities. Though the *quantitative* behavior of the cornea may be to some extent uncertain, its *qualitative* response to environmental variations should be less so. It is useful to examine the implications of these latter type results, in particular, the effect on the corneal potential of substituting choline for sodium on either or both sides of the cornea. In this examination, two qualitative assumptions will be made:

(*a*) The properties of isolated membranes studied by Green are the same as those exhibited by the membranes in his studies of entire corneas. This assumption is supported by his measurements (1967) of unidirectional sodium fluxes across isolated epithelium and whole cornea, and the observed agreement between the SCC and net sodium flux across short-circuited isolated epithelium.

(*b*) The solute permeabilities of the corneal membranes are independent of the composition of the solutions which bound them. Green (private communication) measured the epithelial and endothelial sodium permeabilities when the isolated membranes were bathed on both surfaces with solutions containing 5–118 meq sodium/l (113–0 meq choline/l), and no effect of ambient composition was observed.

The qualitative observations on the corneal potential in vitro are:

(*a*) When sodium is replaced by choline on only the epithelial surface, ψ falls (Muneoka, 1967; Lindemann, 1968; Green, private communication [Fig. 3]).

(*b*) When sodium is replaced by choline on both corneal surfaces, ψ falls, possibly less than in *a* above (Muneoka, 1967).

(*c*) When sodium is replaced by choline on only the endothelial surface, ψ is essentially unchanged (Muneoka, 1967).

The epithelial pump rate may depend with a positive coefficient on the sodium content of the epithelial bath, the endothelial bath, both, or neither; the permeability of the membranes to choline may be much less than, much greater than, or comparable to that to sodium. Of these 12 possibilities, only three are consistent with the potential variations listed above, and, incidentally, with the SCC variations reported by Green (1969). They are:

(*a*) $F_{2k} \approx F_{1k}$ and P decreases as c_{11} is lowered;

(*b*) $F_{2k} \gg F_{1k}$ and P decreases as c_{13} is lowered;

(*c*) $F_{2k} \gg F_{1k}$ and P decreases as c_{11} and/or c_{13} are lowered (P depends on both c_{11} and c_{13}).

The reduction to the three alternatives given above is made without recourse to any numerical permeability or SCC values. When those values reported by Green are used, $F_{2k} \gg F_{1k}$, the pump rate is found to be independent of c_{11}, and hence *b* is indicated. This implies that P depends effectively on the sodium concentration at the posterior surface of the epithelium. Such could be the case if the surface perme-

ability of the epithelium were very low, so that most of the pump substrate enters the transporting cells from the extracellular space.

The differentiation between alternatives *b* and *c* above is made on the basis of the experimental values of SCC and F_{11}; the magnitude of F_{12} is less critical. It can be seen from equation 7 that the calculated pump rate will decrease as c_{11} falls if the SCC falls more rapidly with diminishing c_{11} than is given in Table II, or if F_{11} is larger than the value computed from the parameters in Table I. If the SCC data in choline-free solutions are reliable, the value of F_{11} cannot be much larger than that used here; for cases 1 and 2, SCC is a good enough approximation to P, and the calculated corneal potentials in Fig. 3 would not agree with experiment were a substantially higher epithelial resistance used in the potential calculation.

The alternative *a* above gives the expected dependence of pump rate on ambient composition. Since a principal purpose of this study is the examination of the variation of open-circuit corneal behavior in response to environmental changes, this behavior was examined for the case $F_{2k} = F_{1k}$ even though this equality runs counter to the experimental data in Table I. Cases 4 and 6 were repeated and are compared in Table III with results based on the Table I permeabilities. For consistency, the pump rates were calculated from equation 7 for all cases. It can be seen that alterna-

TABLE III

OPEN-CIRCUIT CORNEAL PARAMETERS AS A FUNCTION OF CHOLINE PERMEABILITY

Parameter	Choline permeability				
	From Table I			Equated to Table I sodium permeability	
	Case 2*	Case 4	Case 6	Case 4	Case 6
P, *eq/cm²-sec* (equation 7)	1.035×10^{-11}	9.82×10^{-11}	9.98×10^{-11}	5.32×10^{-11}‡	1.182×10^{-11}‡
ψ, *mv*	9.1	5.2	1.1	4.7	1.1
ψ (experimental), *mv*	8.1	4.0	0.4	4.0	0.4
Average stromal tonicity, *milliosmols/l*	306.6	303.5	301.1 ± 1.2§	302.6	299.4
Composition of average stromal environment‖					
Na^+, *meq/l*	122.9	120.5	117.7	117.3	111.8
Ch^+, *meq/l*	0	0.6	2.0 ± 0.7§	3.2	6.8

* No choline present.

‡ When sodium and choline permeabilities are identical, $P = \alpha(F_{11} + F_{12})/F_{11}$.

§ Convergence difficulties permitted only a range of values to be found.

‖ Average of subepithelial and supraendothelial solutions.

tives a and b cannot be differentiated on the basis of corneal potential measurements and that the variations of stromal tonicity and sodium content with c_{11} are even more marked when the higher choline permeabilities are used.

The general solution (equation 4) relating P to SCC can be manipulated to yield further insights into the dependence of the calculated corneal pump rate on the SCC and the composition of the ambient baths. It will first be observed that if the cornea is fairly represented as a series system with only one actively transporting membrane, the structured-epithelium case discussed above can also be taken to represent more complex systems, where all resistance anterior to the pumping membrane is lumped in the anterior epithelial membrane and all resistance posterior is lumped in the endothelium. In applying equation 4 to this case, $K = 3$ ($k = 1a, 1p, 2$), $k' = 1p$ and the notation is otherwise unchanged. For $j = 1$ and the limiting case $X_2 \ll \alpha$, an equation corresponding to equation 7 is obtained:

$$P = \frac{1}{F_{1,1p}}\left\{\frac{\mathfrak{S}}{N_1 + \alpha F_{12} + X_2 F_{22} - \alpha F_{1,1a} - X_2 F_{2,1a}}\right\}, \tag{8}$$

where

$$\mathfrak{S} = \alpha[F_{1,1p} + F_{12}][N_1 + \alpha F_{12} + X_2 F_{22}] - N_1[c_{11} - c_{13}]/2$$

$$+ \alpha[F_{1,1a}(N_1 - \alpha F_{1,1a} - X_2 F_{2,1a}) - F_{1,1p}(\alpha F_{1,1a} + X_2 F_{2,1a})].$$

Equation 8 reduces to equation 7 when $F_{j,1a} = 0$ and F_{12} is comparable to F_{22}. For $j = 2$, equation 4 gives a quadratic in X_2, the solution of which can then be substituted into equation 8 to give P.

When the parameters of the structured epithelium used earlier are substituted into equation 8, it is found that setting $X_2 = 0$ in this equation gives values of P in no worse agreement with the computer results than is obtained when X_2 is found from the quadratic, and that the αF_{1k} products may also be dropped where they appear with N_1 without much loss in accuracy. Equation 8 then simplifies considerably to

$$P = \alpha \frac{F_{1c}}{F_{1p}} - \frac{c_{11} - c_{13}}{2F_{1p}}, \tag{9 a}$$

where $F_{1p} = F_{1,1p}$ measures the passive resistance of the pumping membrane to sodium and $F_{1c} = F_{1,1a} + F_{1,1p} + F_{12}$ is the total corneal resistance to the passage of this ion. Equation 9 a gives values of the pump rate in the structured epithelium of 2.21×10^{-10} and 2.13×10^{-10} eq/cm^2-sec for cases 2 and 6, in good agreement with the computer results given in the preceding section. A similarly good agreement with the pump rates in Fig. 2 is obtained when $F_{1p} = F_{11}$.

Equation 9 *a* can be rearranged to give

$$\alpha = \frac{1}{F_{1c}}\left(F_{1p}P - \frac{c_{13}}{2}\right) + \frac{1}{2F_{1c}} \cdot c_{11}. \qquad (9\,b)$$

Thus, if P and the $\{F_{1k}\}$ are independent of c_{11}, with c_{13} fixed, α should be a linear function of c_{11}, with slope $(2F_{1c})^{-1}$. Alternatively, if a plot of α vs. c_{11}, with c_{13} fixed, is linear with a slope of $(2F_{1c})^{-1}$, P is constant if the $\{F_{1k}\}$ are. Equation 9 *b* is plotted in Fig. 2, using $F_{1p} = F_{11}$ and P for unstructured epithelium, and the agreement with Green's (1968, 1969) SCC data is evident. Since the *constancy* of P hinges on only the *over-all* corneal resistance F_{1c} (its constant *value* depends on additional variables, particularly F_{1p}), structural considerations are not influential in this regard. The unimportance of epithelial structure vis-à-vis the constancy of P has been confirmed by further calculations in which the partitioning of diffusional resistance among the epithelial membranes was varied from that indicated by Klyce and Zadunaisky (1970).

Green (1969) observed that a Lineweaver-Burke plot of α^{-1} vs. c_{11}^{-1} was linear and took this as indicative of the behavior of an enzyme system obeying Michaelis-Menten kinetics, with $P = \alpha$. An alternative explanation is evident from equation 9 *b*. The α-intercept given by this equation is only 1.1×10^{-11} eq/cm^2-sec, so α^{-1} is approximately proportional to c_{11}^{-1} for small c_{11}^{-1}. It may be noted that when sulfate Ringer was used in Green's experiments, an (impossible) negative "maximal velocity" was obtained. It is more reasonable to regard the α^{-1}-axis intercepts found by Green in chloride and sulfate Ringer as simply representing experimental scatter about the zero value predicted by equation 9 *b*.

The apparent invariability of P can be viewed in terms of Essig and Caplan's (1968) irreversible thermodynamic description of the energetics of active transport. The transporting membrane contains active and passive (leak) pathways, denoted by the superscripts a and p, respectively. The fluxes of sodium through these paths are $X_1^a = L_1^a\,(-\Delta\tilde{\mu}_1) + L_{1r}^a A$ and $X_1^p = L_1^p\,(-\Delta\tilde{\mu}_1)$, where L_1^i is the "straight" phenomenological coefficient for the ith path coupling the flow of cation to its conjugate force, the electrochemical potential difference $-\Delta\tilde{\mu}_1$ across the membrane, and L_{1r}^a is the coupling coefficient between X_1^a and the affinity A of the metabolic reaction which characterizes the pump. All phenomenological coefficients are positive and ion-ion interactions have been neglected. By definition, $X_1 = X_1^a + X_1^p = L_1\,(-\Delta\tilde{\mu}_1) + L_{1r}^a A$, where $L_1 = L_1^a + L_1^p$. But $L_1(-\Delta\tilde{\mu}_1)$ is the passive flux J_1, that portion of the sodium flux through the pumping membrane attributable to the electrochemical driving force; thus $P = X_1 - J_1 = L_{1r}^a A$. By this definition, the pump flux P represents that flux of actively transported ion which is not directly affected by the driving force for passive flow.

The pump rate may alternatively be regarded as the total flux X_1^a through the

active pathway; $X_1^a = (L_1^a/L_1)J_1 + P$, where $0 < L_1^a/L_1 \leq 1$ and $L_1^a/L_1 = 1$ corresponds to the absence of leak. Thus $X_1 \leq X_1^a < P$. Returning to the corneal experiments, since X_1 falls as c_{11} is reduced, X_1^a can fall as well by an amount dependent on L_1^a/L_1, even though P is unchanged.

CONCLUDING REMARKS

The computer experiments described above lend several new insights into active and passive transport in the isolated cornea. The epithelial pump rate is found to be much less sensitive to the composition of the epithelial bath than was earlier believed, and the stromal tonicity is found to fall as sodium in the epithelial bath is replaced by choline. These observations are not only of interest per se; they also render highly questionable any hypothesis as to the cause of the corneal swelling known to accompany the decrease in ambient sodium, if such hypotheses are based on only electrolyte transport through the tissue. Although the present approach is suitable for the purpose for which it was intended, that is, the study of the transport and electrical properties of series membrane systems bathed in complex media, it is insufficiently complete to describe the hydration behavior of swellable tissue. Fortunately, convection is negligible here, insofar as the solute fluxes are concerned, and the stromal resistance to diffusion is trivial at any thickness, so the electrical and solute transport properties of this tissue are effectively uncoupled from its swelling behavior. It appears that if the effect of ambient composition on the *swelling* behavior of the cornea is to be understood, solvent flow must be taken into account and the composition dependence of the epithelial reflection coefficients and hydraulic conductivity, as well as its solute permeabilities, must be known.

The results of this work support the thesis (Ehlers, 1966; Maurice, 1967; Trenberth and Mishima, 1968) that the epithelial sodium pump cannot act to inhibit corneal swelling. As has already been noted, the consistency of Green's (1969) measurements of the sodium content of posttest swollen stromata with the computer results shows that the decrease in "bound sodium" which accompanies swelling can be explained as a dilution effect. Replacement of sodium by choline in the epithelial bath promotes swelling. The *number* of bound sites in the stroma changes little as the tissue swells, so the *concentration* of bound sites, measured per unit mass stromal fluid, necessarily becomes less.

The author wishes to thank Dr. Keith Green for helpful discussions and unpublished data. Computer programming and execution services were provided by Mary E. Lynam.

This investigation was supported in part by U. S. Public Health Service grant NS 07226 from the National Institute of Neurological Diseases and Stroke.

Received for publication 21 May 1971 and in revised form 3 November 1971.

APPENDIX I

General Donnan Equilibrium Equations

Consider an interface between two phases, identified by single and double primes. The charge density of each phase is known, and the known ionic composition on one side of the interface is given by $c_1', \cdots, c_i', \cdots, c_n'$. All n ions are free to enter either phase. Assume that in each phase, the ionic activity coefficients γ_i are the same for all ions of like sign, and are known. The temperature of the system is uniform, pressure effects on ion activity are neglected, and all ions are monovalent. The space charge region at the interface is assumed to be negligibly small compared with the thickness of the bulk phases. The composition $\{c_i''\}$ is sought.

At equilibrium, the electrochemical potential of each ion is the same in each phase:

$$RT \ln \gamma_i'' c_i'' - RT \ln \gamma_i' c_i' + z_i F \Delta\psi = 0, \tag{A 1}$$

where $\Delta\psi = \psi'' - \psi'$, the Donnan interface potential. Let $E = \exp [z_{x''} F \Delta\psi/(RT)]$. Equation A 1 is solved for c_i'' and the definition of E is used to give

$$c_i'' = (\gamma_i' c_i'/\gamma_i'') E^{-z_i/z_{x''}} \tag{2 a}$$

Since each phase is electrically neutral, $\sum_i z_i c_i'' + z_{x''} X'' = 0$; the first term in the electroneutrality condition can be replaced by $z_{x''} (\sum_{c''} c_i'' - \sum_{g''} c_i'')$, where the index c'' runs over the coions and g'' includes the counterions in the double-primed phase. Dividing by $z_{x''}$, we have, with equation 2 a,

$$-X'' = [\sum_{c''} (\gamma_i' c_i'/\gamma_i'')]/E - E \sum_{g''} (\gamma_i' c_i'/\gamma_i''). \tag{A 2}$$

Equation A 2 can be solved for E, and equation 2 a can be used to find c_i''. It is sometimes convenient, however, to write E in terms of $N' = \sum_i c_i'$; to do this, the electroneutrality condition for the primed phase is used, again classifying ions according to whether they are coions or counterions in the doubly primed phase:

$$z_{x''} (\sum_{c''} c_i' - \sum_{g''} c_i') + z_{x'} X' = 0. \tag{A 3}$$

Since it is assumed that the ion activity coefficients in each phase depend on only the sign of z_i, the summations in the right-hand side of equation A 2 can be written as $(\gamma_i'/\gamma_i'')_{c''} \sum_{c''} c_i' \equiv \Gamma_{c''} \sum_{c''} c_i'$ and $(\gamma_i'/\gamma_i'')_{g''} \sum_{g''} c_i' \equiv \Gamma_{g''} \sum_{g''} c_i'$, respectively. The sums $\sum_{c''} c_i'$ and $\sum_{g''} c_i'$ are found from equation A 3 and the definition of N', written as $N' = \sum_{c''} c_i' + \sum_{g''} c_i'$; equation A 2 becomes

$$-X'' = \Gamma_{c''} (N' - z_{x'} z_{x''} X')/(2E) - E \Gamma_{g''} (N' + z_{x'} z_{x''} X')/2. \tag{A 4}$$

Equation 2 b is the solution of equation A 4.

APPENDIX II

Relations among Pump Currents and Species Fluxes in a Series Membrane System

Consider a short-circuited assembly of K uncharged membranes in series, bathed on its opposing surfaces by multicomponent electrolyte solutions whose compositions in general dif-

fer but whose total concentrations N_1 and N_{K+1} do not. The membranes possess any number of ion pumps, all of which transport ions of like sign, say cations (the roles of cations and anions can be reversed throughout this discussion). There are n cations in the system; P_{jk} is the pump rate of the jth cation through the kth membrane in the direction of increasing k. The anion content of both bathing solutions is identical. Direct ion-ion interactions and convection are neglected, so the anion fluxes are zero.

Under these conditions, the flux and potential equations 1 simplify considerably. When the substitutions $\bar{R} = 0, X = 0$, and $J_j(z_j = -1) = 0$ are made, $\pi_1 = \sum_j f_j J_j = \sum_{j(z_j=-1)} f_j J_j = \sum_j J_j z_j f_j$, whence $\pi_{8j} = z_j$. Equations 1 *a* and 1 *b* then become, for cations in the kth membrane,

$$c_{j,k+1} = \frac{J_{jk} f_{jk}}{2\pi_{1k}} \left(N_{k+1} - \frac{N_k^2}{N_{k+1}} \right) + \left(\frac{N_k}{N_{k+1}} \right) c_{jk}, \qquad \text{(A 5 } a\text{)}$$

$$\frac{a_k}{\overline{RT}} = \frac{N_k - N_{k+1}}{\pi_{1k}}, \qquad \text{(A 5 } b\text{)}$$

where the subscript k on c_j and N refers to those variables at the kth interface, between the kth and $(k-1)$st membranes. The value of π_{1k} given by equation A 5 *b* is substituted into equation A 5 *a* to give

$$c_{j,k+1} = (P_{jk} - X_j) F_{jk} \left(1 + \frac{N_k}{N_{k+1}} \right) + \frac{N_k}{N_{k+1}} c_{jk}, \qquad \text{(A 6)}$$

where $F_{jk} \equiv f_{jk} a_k / (2RT)$ and $X_j = J_{jk} + P_{jk}$ has been used; F_{jk} is proportional to the reciprocal of the permeability of the jth cation in the kth membrane.

In reducing equation A 6 to a practically useful form, it will be assumed that the $\{P_{jk}\}$ are known and the $\{X_j\}$ are not; the inverse problem cannot always be solved, if too many nonzero P_{jk}'s of unknown magnitude are postulated. Equation A 6 is in fact nK equations for n cations across K membranes; the unknowns are $n(K-1)$ c_{jk}'s and $K-1$ N_k's at the internal interfaces, and n X_j's, a total of $nK + K - 1$. An additional $K-1$ equations are provided by the definition of N_k at the internal interfaces;

$$\sum_j c_{jk} = N_k/2 \qquad (k = 2, \cdots, K). \qquad \text{(A 7)}$$

Equation A 6 is of the form $c_{j,k+1} = \alpha_{jk} + \beta_k c_{jk}$, a recurrence relation on c_{jk} which can be used to give $c_{j,k+1}$ in terms of the concentration c_{j1} of the jth ion in the bathing solution at the first membrane, and ultimately to eliminate the internal compositions as unknowns in the formulation:

$$c_{j,k+1} = \alpha_{jk} + \sum_{i=1}^{k-1} \beta_k \cdots \beta_{k-i+1} \alpha_{j,k-i} + c_{j1} \prod_{i=1}^{k} \beta_i. \qquad \text{(A 8)}$$

For $k = K$, $\prod_{i=1}^{K} \beta_i = \prod_{i=1}^{K} (N_i/N_{i+1}) = (N_1/N_2)(N_2/N_3) \cdots (N_{K-1}/N_K)(N_K/N_{K+1}) = N_1/N_{K+1} = 1$, by hypothesis. More generally, $\prod_{i=1}^{k} \beta_i = N_1/N_{k+1}$. Again, for $k = K$, the β product in the second term in the right-hand side of equation A 8 is $\prod_{l=K-i+1}^{K} \beta_l = \prod_{l=1}^{K} \beta_l / \prod_{l=1}^{K-i} \beta_l = N_{K-i+1}/N_1$. Thus

$$c_{j,K+1} = \alpha_{jK} + \sum_{i=1}^{K-1} \frac{N_{K-i+1}}{N_1} \alpha_{j,K-i} + c_{j1}$$

$$= \frac{1}{N_1} \sum_{i=0}^{K-1} s_{j,K-i}(N_{K-i+1} + N_{K-i}) + c_{j1} \qquad (j = 1, \cdots, n), \quad (A\,9)$$

where $\alpha_{jk} = (P_{jk} - X_j)F_{jk}(1 + N_k/N_{k+1}) \equiv s_{jk}(1 + N_k/N_{k+1})$. Equation A 9 constitutes $n - 1$ independent equations in n X_j's and $K - 1$ N_k's; the internal concentrations of the individual cations have been eliminated. The remaining K equations are constructed by summing equation A 6 over j to give

$$\frac{N_{k+1}}{2} = \left(1 + \frac{N_k}{N_{k+1}}\right) S_k + \frac{N_k^2}{2N_{k+1}},$$

where $S_k = \sum_j s_{jk}$; this rearranges to

$$N_{k+1} = 2S_k + N_k \qquad (k = 1, \cdots, K). \qquad (A\,10)$$

It now remains to eliminate the internal total concentrations, $\{N_k\}$. Equation A 10 is a recurrence relation on N_k of the same form as that on c_{jk} , with α_{jk} replaced by $2S_k$ and β_k replaced by unity. Thus,

$$N_{k+1} = 2S_k + 2 \sum_{l=1}^{k-1} S_{k-l} + N_1 = 2 \sum_{l=0}^{k-1} S_{k-l} + N_1. \qquad (A\,11)$$

Equation A 11 is to be substituted into equation A 9 to eliminate the $\{N_k\}$. It will be noted that when $i = K - 1$ in the summation in equation A 9, N_2 and N_1 are called for, but N_1 is not given by equation A 11. Thus the sum in equation A 9 is broken into $i = 0, \cdots, K - 2$ and $i = K - 1$, and equation A 10 with $k = 1$ is used for the latter. The implication is that $K > 1$; for $K = 1$, equation A 9 reduces directly to $c_{j2} - c_{j1} = 2s_{j1}$. After a convenient change in indexing, the final equation is

$$c_{j,K+1} - c_{j1} = \frac{2}{N_1}\left[\sum_{k=1}^{K} s_{jk}(N_1 + S_k) + 2 \sum_{k=2}^{K} s_{jk} \sum_{l=1}^{k-1} S_l\right] \qquad (j = 1, \cdots, n). \quad (3)$$

These n equations can in principle be solved for the n gross species fluxes $\{X_j\}$ and the SCC $\sum_j X_j$ if the pump array $\{P_{jk}\}$ is given.

Special Case: Determination of a Single Pump Rate from SCC Data

For the present purpose, it is convenient to specialize this set (equation 3) of coupled second-degree equations to the case in which only a single pump is present. Assume the single non-zero pump rate is $P_{j'k'} = P$ and that the SCC is to be used to find its value. The sums $\sum_{k=1,2}^{K}$ are broken into three terms: $\sum_{k=1,2}^{k'-1}$, $k = k'$, and $\sum_{k=k'+1}^{K}$. Define $S_0 \equiv 0$. Then equation 3 becomes

$$\begin{aligned} c_{j,K+1} - c_{j1} = \frac{2}{N_1}\Bigg[& \delta_{k'>1} \sum_{k=1}^{k'-1} s_{jk}\left(N_1 + S_k + 2 \sum_{l=0}^{k-1} S_l\right) \\ & + s_{jk'}\left(N_1 + S_{k'} + 2 \sum_{l=0}^{k'-1} S_l\right) \\ & + \delta_{k'<K} \sum_{k=k'+1}^{K} s_{jk}\left(N_1 + S_k + 2 \sum_{l=0}^{k-1} S_l\right)\Bigg], \quad (A\,12) \end{aligned}$$

where $\delta_{k'>1}$ is unity if $k' > 1$ and zero if $k' = 1$, and similarly for $\delta_{k'<K}$. The solution for P is facilitated if equation A 12 is rewritten in a form such that the unknown pump rate appears on the right-hand side only when $j = j'$, and then only linearly. In the form given above, this condition is not satisfied by the $s_{jk'}S_{k'}$ product in the $k = k'$ term, or the $\sum_{k=k'+1}^{K} s_{jk} \cdot \sum_{l=0}^{k-1} S_l$ double sum in the last term, because P appears in $S_{k'}$. From equation A 11, with $k = K$, it is seen that $\sum_{l=1}^{K} S_l = 0$, since $N_{K+1} = N_1$; thus $S_{k'}$ may be replaced by a sum of S's from which P is absent. Defining $S_{K+1} \equiv 0$,

$$c_{j,K+1} - c_{j1} = \frac{2}{N_1}\left[\delta_{k'>1}\sum_{k=1}^{k'-1} s_{jk}\left(N_1 + S_k + 2\sum_{l=0}^{k-1} S_l\right)\right.$$
$$+ s_{jk'}\left(N_1 + \sum_{l=0}^{k'-1} S_l - \sum_{l=k'+1}^{K+1} S_l\right)$$
$$\left. + \delta_{k'<K}\sum_{k=k'+1}^{K} s_{jk}\left(N_1 + S_k - 2\sum_{l=k}^{K} S_l\right)\right]. \quad (4)$$

REFERENCES

BROWN, K. M., and S. D. CONTE, 1967. *Proc. Ass. Comput. Mach. 22nd Nat. Conf.* P-67:111.
CATCHPOLE, H. R., N. R. JOSEPH, and M. B. ENGLE. 1966. *Fed. Proc.* 25:1124.
CEREIJIDO, M., and P. F. CURRAN. 1965. *J. Gen. Physiol.* 48:543.
DONN, A., D. M. MAURICE, and N. L. MILLS. 1959. *Arch. Ophthalmol.* 62:748.
DONN, A., S. L. MILLER, and N. N. MALLETT. 1963. *Arch. Ophthalmol.* 70:515.
EDELHAUSER, H. F., J. R. HOFFERT, and P. O. FROMM. 1968. *Amer. J. Physiol.* 214:389.
EDSALL, J. T., and J. WYMAN. 1958. Biophysical Chemistry. Academic Press, Inc., New York. 1:399.
EHLERS, N. 1966. *Dan. Med. Bull.* 13:133.
EHLERS, N., and D. EHLERS. 1968. *Acta Ophthalmol.* 46:767.
ESSIG, A., and S. R. CAPLAN. 1968. *Biophys. J.* 8:1434.
FRIEDMAN, E., and C. KUPFER. 1960. *Arch. Ophthalmol.* 64:892.
FRIEDMAN, M. H. 1970. *Biophys. J.* 10:1013.
FRIEDMAN, M. H., and K. GREEN. 1971. *Amer. J. Physiol.* 221:356.
GREEN, K. 1967. *Exp. Eye Res.* 6:79.
GREEN, K. 1968. *Nature (London).* 217:1074.
GREEN, K. 1969. *Amer. J. Physiol.* 217:1169.
GREEN, K., B. HASTINGS, and M. H. FRIEDMAN. 1971. *Amer. J. Physiol.* 220:520.
KATCHALSKY, A., and P. F. CURRAN, 1965. Nonequilibrium Thermodynamics in Biophysics. Harvard University Press, Cambridge, Mass. 133.
KEDEM, O., and A. KATCHALSKY. 1961. *J. Gen. Physiol.* 45:143.
KLYCE, S. D., and J. A. ZADUNAISKY. 1970. *Biophys. Soc. Annu. Meet. Abstr.* 10:199a.
LEAF, A. 1960. *J. Gen. Physiol.* 43:(Suppl.)175.
LINDEMANN, B. 1968. *Exp. Eye Res.* 7:62.
MAURICE, D. M. 1961. *In* Structure of the Eye. G. Smelser, editor. Academic Press, Inc., New York. 381.
MAURICE, D. M. 1962. *In* The Eye. H. Davson, editor. Academic Press, Inc., New York. 1:289.
MAURICE, D. M. 1967. *Exp. Eye Res.* 6:138.
MUNEOKA, A. 1967. *Nippon Ganka Gakkai Zasshi (J. Jap. Ophthalmol. Soc.).* 71:1095.
OTORI, T. 1967. *Exp. Eye Res.* 6:356.
REHM, W. S. 1968. *J. Theor. Biol.* 20:341.
TEORELL, T. 1953. *Progr. Biophys. Biophys. Chem.* 3:305.
TRENBERTH, S. M., and S. MISHIMA. 1968. *Invest. Ophthalmol.* 7:44.
USSING, H. H. 1960. *J. Gen. Physiol.* 43:(Suppl.)135.